Matrix Factorization-Based Target Localization via Range Measurements With Uncertainty in Transmit Power

Xiaojun Mei, *Graduate Student Member, IEEE*, Huafeng Wu, *Senior Member, IEEE*, and Jiangfeng Xian

***Abstract*—In this letter, received signal strength (RSS)- based target localization with uncertainty in transmit power (UTP) is studied. First, the localization-based alternating nonnegative constrained least squares (ANCLS) framework is conducted. A two-phase optimization method, i.e., a matrix factorization-based min-max strategy (MFMM), is then presented to figure out the solution. The first phase of optimization is based on a matrix factorization approach, i.e., active set method (ASM). However, ASM may drop to a local minimum. Therefore, a min-max strategy based on a Taylor linearization approximation is involved in the second phase, where the objective is split into a convex quadratic and a concave term. The target position and UTP are refined simultaneously in the iteration via solving a sequence of convex problems, in which the solution obtained by ASM is to be the initiation. Additionally, to evaluate the effectiveness of MFMM, both the computational complexity and the Cramer-Rao lower bound (CRLB) are analyzed. Simulations are carried out to illustrate the outperformance, compared with other state-of-the-art methods in different scenarios.**

***Index Terms*—Received signal strength (RSS), min-max strategy, target localization, nonnegative matrix factorization (NMF), uncertain transmit power, Cramer-Rao lower bound (CRLB).**

I. Introduction

TARGET localization has been drawn much attention in both military and industrial applications [1], where the data collected by sensors or other facilities are meaningful only when the latter is appropriately geo-referenced [2]. Together with the benefit of cost-effective and synchronization-free among the localization techniques, received signal strength (RSS) has attracted researchers to explore in the literature compared with time of arrival (TOA), time difference of arrival (TDOA), and angle of arrival (AOA) [3]. A considerable body of research has been done concerning target localization using RSS measurements [4]–[12], which drives a notable advance to target localization [13], [14].

Nevertheless, it is worth noting that most research is studied in the assumption of known transmit power (TP), which is not practical in many situations. Therefore, various suboptimal estimators have been derived for the unknown transmit power (UTP) case, for instance, [4], [7], [9]. Notwithstanding, either of them may have poor performance or surfer high computational complexity. This leads to the motivation of this letter, where a computationally light method, i.e., a matrix factorization-based min-max strategy (MFMM), is proposed on the premise of localization accuracy. The localization problem is solved under an alternating nonnegative constrained least squares (ANCLS) framework, wherein an active set method (ASM) incorporated with a min-max strategy is developed to acquire the optimum and improve the performance.

The main contributions of this letter could be concluded as two parts: 1) An ANCLS framework is conducted to avoid a substantial computational complexity due to the absence of TP and the characteristic of highly non-convex in the problem. 2) A two-phase optimization method, i.e., MFMM, is presented to solve the problem, wherein the first is in the ASM, and the second is in the min-max strategy.

II. Problem Formulation

Consider a k-dimensional ($k = 2$ or 3) sensor network with M anchor nodes that are aware of their positions and a target whose position needs to be determined. The position of the target is $\boldsymbol{x} = [x_1, \ldots, x_k]^T$, and the position of the i^{th} anchor node is $\boldsymbol{a}_i = [a_{i1}, \ldots, a_{ik}]^T$, wherein $i = 1, \ldots, M$ and T represents the transpose operation. We assume that the target could transmit the radio signal with RSS information to anchors, of which the signal is modeled as [5]

$$P_{ri} = P_0 - 10\alpha \log_{10} \frac{\|\boldsymbol{x} - \boldsymbol{a}_i\|}{d_0} + \eta_i \tag{1}$$

where P_{ri} denotes the received signal power of the i^{th} anchor node from the target, d_0 is a reference distance ($\|\boldsymbol{x} - \boldsymbol{a}_i\| \geq d_0$), P_0 is the transmit power of the target in terms of d_0, α represents the path loss exponent, $\|\cdot\|$ is the ℓ_2 norm, and η_i is the measurement noise modeled as Gaussian distribution: $\eta_i \sim \mathcal{N}(0, \sigma_i^2)$.

Manuscript received April 20, 2020; revised May 17, 2020; accepted May 26, 2020. Date of publication May 29, 2020; date of current version October 7, 2020. This work was supported in part by the Shanghai Committee of Science and Technology, China, under Grant 18040501700, in part by the National Natural Science Foundation of China under Grant 51579143, Grant 61701299, and Grant 51709167, in part by the Ministry of Education of Humanities and Social Science Project under Grant 15YJC630145, in part by the Top-Notch Innovative Program for Postgraduates of Shanghai Maritime University under Grant 2019YBR002 and Grant 2019YBR006, in part by the Postgraduate Innovation Foundation of Shanghai Maritime University under Grant 2017ycx030 and Grant 2016ycx042, and in part by the China Scholarship Council. The associate editor coordinating the review of this article and approving it for publication was Y. Shen. *(Corresponding authors: Xiaojun Mei; Huafeng Wu.)*

Xiaojun Mei is with the Merchant Marine College, Shanghai Maritime University, Shanghai 201306, China, and also with the Institute for Systems and Robotics, Instituto Superior Técnico, University of Lisbon, Lisbon 049-001, Portugal (e-mail: xjmei94@163.com).

Huafeng Wu is with the Merchant Marine College, Shanghai Maritime University, Shanghai 201306, China (e-mail: hfwu@shmtu.edu.cn).

Jiangfeng Xian is with the Merchant Marine College, Shanghai Maritime University, Shanghai 201306, China, and also with the Department of Electronics and Telecommunications, Politecnico di Torino, 10129 Torino, Italy (e-mail: xianjiangfeng0310@163.com).

Digital Object Identifier 10.1109/LWC.2020.2998609

III. Proposed Localization Approach

A. ANCLS Framework

Given the observation vector $\boldsymbol{P} = [P_{ri}]^T$, the probability density function (PDF) under UTP is given as

$$p(\boldsymbol{P}|\boldsymbol{x}, P_0) = \prod_{i=1}^{M} \frac{1}{\sqrt{2\pi\sigma_i^2}} \exp\left\{ \frac{\left(P_{ri} - P_0 + 10\alpha \log_{10} \frac{\|\boldsymbol{x}-\boldsymbol{a_i}\|}{d_0}\right)^2}{2\sigma_i^2} \right\}. \quad (2)$$

By maximizing the joint PDF, the maximum likelihood (ML) estimator of $\boldsymbol{x}$ and P_0 is derived as

$$F\left(\hat{\boldsymbol{x}}, \hat{P}_0\right) = \arg\min_{\boldsymbol{x}} \sum_{i=1}^{M} \frac{\left(P_{ri} - P_0 + 10\alpha \log_{10} \frac{\|\boldsymbol{x}-\boldsymbol{a_i}\|}{d_0}\right)^2}{2\sigma_i^2}. \quad (3)$$

However, it is quite challenging to solve the problem in the absence of TP with a substantial computational complexity due to its highly non-convex. In this case, we develop a novel method with less computation under the ANCLS framework.

Firstly, a transformation is derived by applying the simple manipulations from (1) when the noise power is sufficiently small [4].

$$d_0 10^{\mu_i} \approx \|\boldsymbol{x} - \boldsymbol{a_i}\|, \quad (4)$$

where $\mu_i = \frac{P_0 - P_{ri}}{10\alpha}$.

Given the assumption that $\sigma_i = \sigma$, the problem in (3) could be converted into (5).

$$\arg\min_{\boldsymbol{x}} \sum_{i=1}^{M} (d_0 10^{\mu_i} - \|\boldsymbol{x} - \boldsymbol{a_i}\|)^2. \quad (5)$$

Further transformation after squaring range is derived as

$$\arg\min_{\boldsymbol{x}} \sum_{i=1}^{M} \left(d_0^2 10^{2\mu_i} - \chi + 2\mathrm{a}_i^T \boldsymbol{x} - \|\boldsymbol{a_i}\|^2 \right)^2, \quad (6)$$

where $\chi = \|\boldsymbol{x}\|^2$.

Let $\boldsymbol{\theta} = [x_1, \ldots, x_k, 10^{\frac{P_0}{5\alpha}}, \chi]^T$ be the estimated parameter. Then, the problem in (6) is transformed into (7).

$$\arg\min_{\boldsymbol{\theta} \geq 0} \|\boldsymbol{A\theta} - \boldsymbol{B}\|^2, \quad (7)$$

where

$$\boldsymbol{A} = \begin{bmatrix} 2a_1^T & d_0^2 10^{\frac{-P_{r1}}{5\alpha}} & -1 \\ \vdots & \vdots & \vdots \\ 2a_M^T & d_0^2 10^{\frac{-P_{rM}}{5\alpha}} & -1 \end{bmatrix}, \ \boldsymbol{B} = \begin{bmatrix} \|a_1\|^2 \\ \vdots \\ \|a_M\|^2 \end{bmatrix}. \quad (8)$$

With the constraint of $\boldsymbol{\theta}$, i.e., $\boldsymbol{\theta} \geq 0$, which would be released in part *C* with a min-max strategy, the original problem in (3) could be reshaped to the ANCLS framework with a single right-hand side (RHS) vector [15].

B. ASM

ASM is a mathematically rigorous method for ANCLS, which could achieve a relatively high accuracy solution within a finite number of iterations compared with others [16]. In this part, ASM is introduced to solve the RSS localization-based ANCLS.

Algorithm 1 First Phase of MFMM

1. **Initiation:** $\boldsymbol{\theta} = \boldsymbol{0}_{(k+2)\times 1}$, $U = \{1, 2, \ldots, k, k+1, k+2\}$, $C = \emptyset$, $\boldsymbol{\omega} = \boldsymbol{A}^T(\boldsymbol{B} - \boldsymbol{A\theta})$
2. **If** ($U \neq \emptyset$ and $\exists\ j \in U$ with $\omega_j > 0$) **do**
3. Find an index $q \in U$ subject to $\omega_q = max\{\omega_j : j \in U\}$
4. Move the index q from the set U to the set C
5. Figure out the solution of (9) defined by (10)
6. **If** ($\boldsymbol{z}_j \leq 0$ for any $j \in C$) **do**
7. Find an index $t \in C$ with (11)
8. Move from the set C to the set U for all indices $j \in C$ such that $\boldsymbol{\theta}_j = 0$
9. Figure out the solution of (9) defined by (10)
10. **End**
11. $\boldsymbol{\theta} = \boldsymbol{z}$ and $\boldsymbol{\omega} = \boldsymbol{A}^T(\boldsymbol{B} - \boldsymbol{A\theta})$
12. **End**

Let $f = \{1, 2, \ldots, k, k+1, k+2\}$ be the set, wherein each value indexes the columns of $\boldsymbol{A}$ and the rows of $\boldsymbol{\theta}$, and two subsets of $\boldsymbol{A}$ named the active set U and the passive set $\boldsymbol{C}$, where $U \cup C = f$.

Suppose there exist a vector $\boldsymbol{r} \in \mathbb{R}^{(k+\mathbf{2})\times \mathbf{1}}$ and a partition of the integers 1 through $(k+2)$ into subsets U and $\boldsymbol{C}$ with subject to $\boldsymbol{r} = \boldsymbol{A}^T(\boldsymbol{A\theta} - \boldsymbol{B})$, of which the dual vector can be expressed as $\boldsymbol{\omega} = -\boldsymbol{r} = \boldsymbol{A}^T(\boldsymbol{B} - \boldsymbol{A\theta})$. The algorithm contains an outer loop and an inner loop. In what concerns the outer loop step, we should figure out the solution of (9).

$$\arg\min_{\boldsymbol{z}} \|\boldsymbol{A}_C \boldsymbol{z} - \boldsymbol{B}\|, \quad (9)$$

where $\boldsymbol{A}_C$ is the $M \times (k+2)$ matrix defined by (10),

$$\text{column } j \text{ of } \boldsymbol{A}_C = \begin{cases} \text{column } j \text{ of } \boldsymbol{A}, & \text{if } j \in C \\ 0, & \text{if } j \in U \end{cases}, \quad (10)$$

j denotes the value of the set $\boldsymbol{C}$, and $\boldsymbol{z}$ is the potential solution, a $(k+2) \times 1$ vector, in (9).

Besides, in the outer loop, we need to find an index $q \in U$ subject to $\omega_q = max\{\omega_j : j \in U\}$, and move the index q from the set U to the set $\boldsymbol{C}$.

In the inner loop, the new index $t \in C$ needs to be acquired by (11).

$$\begin{aligned} \boldsymbol{\theta}_t/(\boldsymbol{\theta}_t - \boldsymbol{z}_t) &= \min\{\boldsymbol{\theta}_j/(\boldsymbol{\theta}_j - z_j) : \boldsymbol{z}_j \leq 0, j \in C\}, \\ \beta &= \boldsymbol{\theta}_t/(\boldsymbol{\theta}_t - z_t), \\ \boldsymbol{z} &= \boldsymbol{\theta} + \beta(\boldsymbol{z} - \boldsymbol{\theta}). \end{aligned} \quad (11)$$

With the exchange process from the set $\boldsymbol{C}$ to the set U for all indices $j \in C$ such that $\boldsymbol{\theta}_j = \boldsymbol{0}_{(k+2)\times 1}$, the new solution of (9) is obtained. The whole procedure could be concluded in **Algorithm 1**.

C. Min-Max Strategy

However, ASM performs well only the constraint is satisfied, for instance, falling on the first quadrant of a Cartesian coordinate system in 2-Dimension ($k = 2$). Otherwise, the solution may drop in a local optimum, referred to as Fig. 1. Thus, a min-max strategy is presented to drive the local optimum to approach the global optimum, where the start point is the solution acquired by ASM.

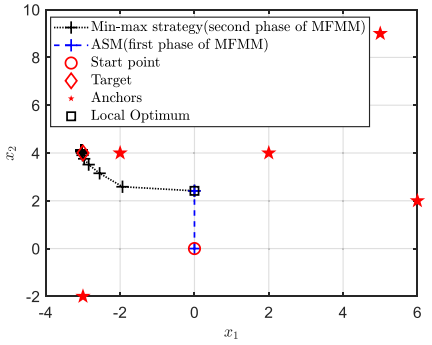

Fig. 1. Convergence analysis where the target $\boldsymbol{x} = [-3, 4]^{\mathrm{T}}$ and anchors $a_1 = [2, 4]^{\mathrm{T}}$, $a_2 = [5, 9]^{\mathrm{T}}$, $a_3 = [-3, -2]^{\mathrm{T}}$, $a_4 = [6, 2]^{\mathrm{T}}$, and $a_5 = [-2, 4]^{\mathrm{T}}$ respectively.

Recall the problem in (5), it could be expressed as (12) after dropping the constant item [17].

$$\arg\min_{\boldsymbol{x}, P_0} \sum_{i=1}^{M} \left(\|\boldsymbol{x} - \boldsymbol{a_i}\|^2 - 2 d_0 10^{\mu_i} \|\boldsymbol{x} - \boldsymbol{a_i}\| \right). \quad (12)$$

Further, a surrogate function is acquired as

$$S(\boldsymbol{x}, P_0) = \underbrace{\sum_{i=1}^{M} \|\boldsymbol{x} - \boldsymbol{a_i}\|^2}_{f(\boldsymbol{x})} + \underbrace{\left(-2 \sum_{i=1}^{M} d_0 10^{\mu_i} \|\boldsymbol{x} - \boldsymbol{a_i}\| \right)}_{g(\boldsymbol{x})}, \quad (13)$$

where the former is convex, and the latter is concave.

Geometrically, the concave function $g(\boldsymbol{x})$ has an upper bound by linearization at $\boldsymbol{x}^Z$, wherein Z is the number of iteration, via first-order Taylor expansion[1] [18].

$$g(\boldsymbol{x}) \le g\left(\boldsymbol{x}^Z\right) + \nabla\, g\left(\boldsymbol{x}^Z\right)^T \left(\boldsymbol{x} - \boldsymbol{x}^Z\right). \quad (14)$$

Thus, by maximizing $g(\boldsymbol{x})$, the objective $S(\boldsymbol{x}|\boldsymbol{x}^Z, P_0^Z)$ is conducted as

$$S\left(\boldsymbol{x}\middle|\boldsymbol{x}^Z, P_0^Z\right) = \sum_{i=1}^{M} \left(\|\boldsymbol{x} - \boldsymbol{a_i}\|^2 - 2 d_0 10^{\mu_i} \left\| \boldsymbol{x}^Z - \boldsymbol{a_i} \right\| \right) - 2 \sum_{i=1}^{M} d_0 10^{\mu_i} \frac{\left(\boldsymbol{x}^Z - \boldsymbol{a_i}\right)^T}{\left\|\boldsymbol{x}^Z - \boldsymbol{a_i}\right\|} \left(\boldsymbol{x} - \boldsymbol{x}^Z\right). \quad (15)$$

Here, we fix P_0 obtained from ASM as P_0^Z, and the update rule for $\boldsymbol{x}^{Z+1}$ as shown in (16).

$$\boldsymbol{x}^{Z+1} = \frac{1}{M} \sum_{i=1}^{M} \left(\boldsymbol{a_i} + d_0 10^{\mu_i} \frac{\left(\boldsymbol{x}^Z - \boldsymbol{a_i}\right)^T}{\left\|\boldsymbol{x}^Z - \boldsymbol{a_i}\right\|} \right). \quad (16)$$

After we obtain $\boldsymbol{x}^{Z+1}$, P_0^{Z+1}could be derived.

$$P_0^{Z+1} = 10\alpha \cdot \frac{1}{M} \sum_{i=1}^{M} \left(\log_{10} \frac{\left\|\boldsymbol{x}^{Z+1} - \boldsymbol{a_i}\right\|}{d_0} + P_{ri} \right). \quad (17)$$

Two conditions should be satisfied in terms of the convergence: 1) The objective $S(\boldsymbol{x}, P_0)$ is bounded below;

[1]It should be noted that (14) holds when $\|\boldsymbol{x} - \boldsymbol{x}^Z\|$ is in a trust region [19], [20], i.e., $\|\boldsymbol{x} - \boldsymbol{x}^Z\| \le \Delta_Z$, where $\Delta_Z > 0$ is the trust region bound at the Z^{th} iteration.

Algorithm 2 Second Phase of MFMM

1. **Input:** $\boldsymbol{x}$ and P_0 obtained from **Algorithm 1**
2. **Initiation:** $\boldsymbol{x}^1 \leftarrow \boldsymbol{x}$, $P_0^1 \leftarrow P_0$ and $Z \leftarrow 1$
3. **While** $(Z < I)$ **do**
4. Update $\boldsymbol{x}^{Z+1}$ according to (16)
5. Update P_0^{Z+1} according to (17)
6. **End while**
7. **Output:** $\boldsymbol{x} \leftarrow \boldsymbol{x}^I$ and $P_0 \leftarrow P_0^I$

2) The objective is non-increasing, i.e., $S(\boldsymbol{x}^{Z+1}, P_0^{Z+1}) \le S(\boldsymbol{x}^Z, P_0^Z)$, and convergences to a limit S^*.

We firstly use $\boldsymbol{\gamma} = [\boldsymbol{x}, P_0]^T$ to be the estimated parameters in the function.

Proof 1): According to the formula (13), one has $S(\boldsymbol{\gamma}) + \sum_{i=1}^{M} d_0^2 10^{2\mu_i} \ge 0$, i.e., $S(\boldsymbol{\gamma}) \ge -\sum_{i=1}^{M} d_0^2 10^{2\mu_i}$, which proves the first condition: The function is bounded below. ■

Proof 2): $S(\boldsymbol{x}, P_0)$ is a surrogate function comprised of a convex term and a concave term. Therefore, the function has an upper bound property that

$$S\left(\boldsymbol{\gamma}\middle|\boldsymbol{\gamma}^Z\right) - S(\boldsymbol{\gamma}) \ge S\left(\boldsymbol{\gamma}^Z\middle|\boldsymbol{\gamma}^Z\right) - S\left(\boldsymbol{\gamma}^Z\right). \quad (18)$$

Because

$$S\left(\boldsymbol{\gamma}\middle|\boldsymbol{\gamma}^Z\right) - S(\boldsymbol{\gamma}) = g\left(\boldsymbol{\gamma}^Z\right) + \nabla^T g\left(\boldsymbol{\gamma}^Z\right)\left(\boldsymbol{\gamma} - \boldsymbol{\gamma}^Z\right) - g(\boldsymbol{\gamma}), \quad (19)$$

where $g(\cdot)$ is the concave term of the function.

Assume $\phi = S(\boldsymbol{\gamma}|\boldsymbol{\gamma}^Z) - S(\boldsymbol{\gamma})$, apparently, ϕ is convex due to the component of an affine function plus a convex term. Thus, $\nabla\phi|_{\boldsymbol{\gamma}=\boldsymbol{\gamma}^Z} = 0$. Then the function is non-increasing and convergence to a limit point, i.e.,

$$S\left(\boldsymbol{\gamma}^{Z+1}\right) \le S\left(\boldsymbol{\gamma}^{Z+1}|\boldsymbol{\gamma}^Z\right) - c^Z \le S\left(\boldsymbol{\gamma}^Z|\boldsymbol{\gamma}^Z\right) - c^Z \le S\left(\boldsymbol{\gamma}^Z\right) = S^*, \quad (20)$$

where $c^Z = S(\boldsymbol{\gamma}^Z|\boldsymbol{\gamma}^Z) - S(\boldsymbol{\gamma}^Z)$. ■

Let the maximum number of iterations be *I*, the pseudocode and the convergence analysis are shown in **Algorithm 2** and Fig. 1, respectively.

D. Cramer-Rao Lower Bound (CRLB) and Complexity Analysis

1) CRLB: In this part, CRLB is conducted in terms of the RSS model to provide the benchmark [21].

The CRLB could be indicated as the trace of the inverse of the Fisher information matrix (FIM), i.e.,

$$CRLB \triangleq Tr\left(FIM^{-1}\right) = Tr\left[\left(\frac{\partial F}{\partial \boldsymbol{\theta}}\right)^T \Sigma^{-1} \left(\frac{\partial F}{\partial \boldsymbol{\theta}}\right)\right]^{-1}, \quad (21)$$

where $\Sigma = \sigma^2$, and

$$\frac{\partial F}{\partial \theta_i} = \left(\xi \cdot \frac{x_1 - a_{i1}}{\|\boldsymbol{x} - \boldsymbol{a_i}\|}, \ldots, \xi \cdot \frac{x_k - a_{ik}}{\|\boldsymbol{x} - \boldsymbol{a_i}\|}, 1 \right) \text{ with } \xi = \frac{10\alpha}{\ln 10 \|\boldsymbol{x} - \boldsymbol{a_i}\|}.$$

Therefore, FIM could be rewritten as

$$FIM = \Sigma^{-1} \begin{bmatrix} \sum_{i=1}^{M} \xi^2 \frac{(x_1 - a_{i1})^2}{\|\boldsymbol{x} - \boldsymbol{a_i}\|^2} & \cdots & \sum_{i=1}^{M} \xi^2 \frac{(x_1 - a_{i1})(x_k - a_{ik})}{\|\boldsymbol{x} - \boldsymbol{a_i}\|^2} & \sum_{i=1}^{M} \xi \frac{x_1 - a_{i1}}{\|\boldsymbol{x} - \boldsymbol{a_i}\|} \\ \vdots & \ddots & \vdots & \vdots \\ \sum_{i=1}^{M} \xi^2 \frac{(x_1 - a_{i1})(x_k - a_{ik})}{\|\boldsymbol{x} - \boldsymbol{a_i}\|^2} & \cdots & \sum_{i=1}^{M} \xi^2 \frac{(x_k - a_{ik})^2}{\|\boldsymbol{x} - \boldsymbol{a_i}\|^2} & \sum_{i=1}^{M} \xi \frac{x_k - a_{ik}}{\|\boldsymbol{x} - \boldsymbol{a_i}\|} \\ \sum_{i=1}^{M} \xi \frac{x_1 - a_{i1}}{\|\boldsymbol{x} - \boldsymbol{a_i}\|} & \cdots & \sum_{i=1}^{M} \xi \frac{x_k - a_{ik}}{\|\boldsymbol{x} - \boldsymbol{a_i}\|} & M \end{bmatrix}. \quad (22)$$

TABLE I
SUMMARY OF THE CONSIDERED METHODS

Method	Complexity
SRWLS [4]	$O(I{\cdot}M)$
RNLA [5]	$O(I{\cdot}M)$
LS [12]	$O(M)$
RSS-SDP [9]	$O(M^{3.5})$
MFMM (proposed)	$O(M{+}I)$

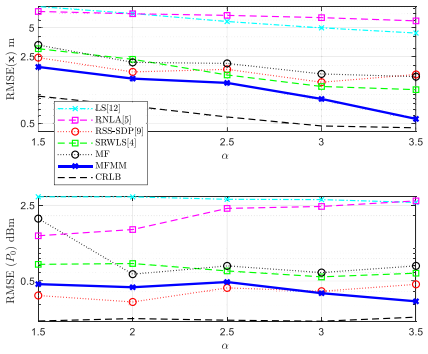

Fig. 2. RMSE for $\boldsymbol{x}$ and P_0 versus variable α with SNR $=$ 40dB and 8 anchors.

2) Computational Complexity: In MFMM, the ASM is the process of solving the LS problem, whose computational complexity is linear in M. Suppose I is the maximum number of iterations in the min-max strategy, the computational complexity of MFMM is $O(M + I)$. Assume the worst computational complexity, Table I provides a summary of the considered algorithms, including squared range weighted least square (SRWLS) in [4], robust localization algorithm (RNLA) in [5], least square (LS) in [12] and RSS-based semidefinite programming (SDP) in [9].

IV. NUMERICAL SIMULATION

In this section, several simulations are carried out to evaluate the performance of MFMM. All algorithms are executed in MATLAB with 2-Dimension ($k = 2$). The position of the target and the anchor nodes are deployed randomly at each Monte Carlo trial. The maximum number of iterations $I = 1000$, $d_0 = 1$ m, and the area is 35×35 m in the simulation. As the calibration for the performance, root mean square error (RMSE) is conducted.

$$RMSE_{position} = \sqrt{\frac{1}{MC}\sum_{nu=1}^{MC}(\widehat{\boldsymbol{x}}-\boldsymbol{x})^2}, RMSE_{UTP} = \sqrt{\frac{1}{MC}\sum_{nu=1}^{MC}\left(\hat{P}_0-P_0\right)^2}, \tag{23}$$

where MC is the number of Monte Carlo trials (we set 1000 in the simulations), $\widehat{\boldsymbol{x}}$ and $\hat{P}$ are the estimates, and nu is the index of MC.

When it comes to the simulations of the cumulative distribution function (CDF) of the algorithms and RMSE versus variable α, SNR, and anchors, the signal-noise ratio (SNR) holds $SNR = 10 \cdot \log_{10}(\|\boldsymbol{x} - \boldsymbol{a}_i\|/(M\sigma^2))$ [4], referred to as Fig. 1 to Fig. 5. However, to study the adverse effect of noise on localization intuitively, the relationship between SNR and σ^2 does not hold in the simulation of RMSE versus variable σ^2, referred to as Fig. 6. Besides, to demonstrate the effectiveness of the min-max strategy, ASM is developed to compare with the related algorithms in the simulations. It should be noted that, in the simulations, we use the mean of CRLB due to the random deployment of anchors and the target at each Monte Carlo trial, i.e.,

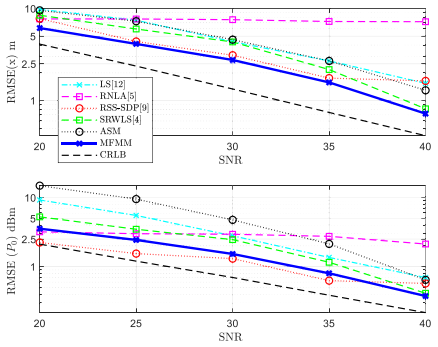

Fig. 3. RMSE for $\boldsymbol{x}$ and P_0 versus variable SNR with $\alpha = 3.5$ and 8 anchors.

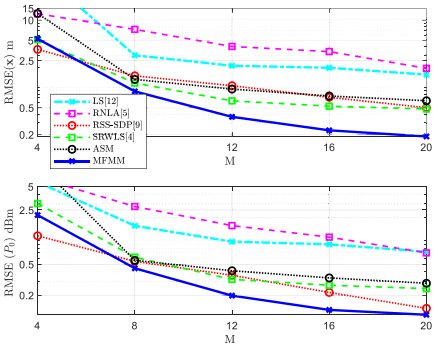

Fig. 4. RMSE for $\boldsymbol{x}$ and P_0 versus variable anchors with $\alpha = 3.5$, SNR $=$ 40 dB.

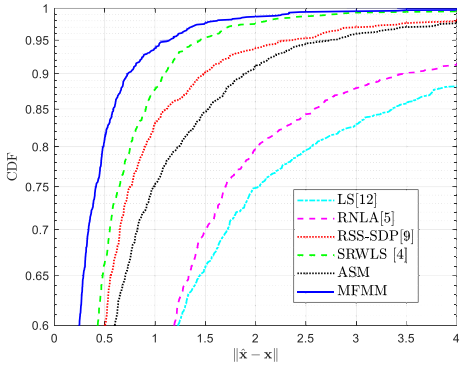

Fig. 5. CDF of $\|\widehat{\boldsymbol{x}} - \boldsymbol{x}\|$ with $\alpha = 3.5$, SNR $=$ 40 dB, and 8 anchors.

$$RMSE_{CRLB} = \sqrt{\frac{1}{MC}\sum_{nu=1}^{MC} CRLB_{nu}} \tag{24}$$

where $CRLB_{nu}$ is the corresponding value at each Monte Carlo trial.

The results of the RMSE versus variable α is shown in Fig. 2. Interestingly, all approaches have relatively acceptable robustness on the rise in path loss exponent, in which MFMM outperforms the others in most cases. Although the performance of the estimate of P_0 in MFMM is worse than that of RSS-SDP when $\alpha < 3$, the estimate of $\boldsymbol{x}$ in MFMM is better than that of RSS-SDP. As for ASM, without the second phase of optimization, the performance is only better than LS and RNLA.

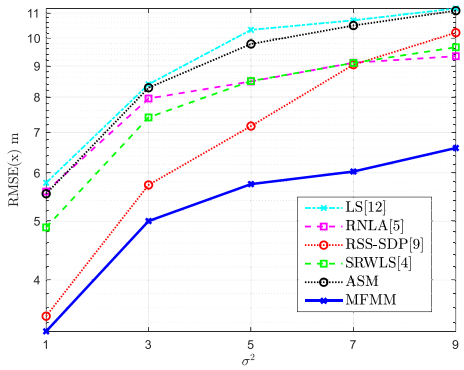

Fig. 6. RMSE for $\boldsymbol{x}$ versus variable σ^2 with $\alpha = 3.5$ and 8 anchors.

The RMSE versus variable SNR is shown in Fig. 3. As expected, the performance of all algorithms is improved when SNR grows. Nevertheless, similar results are performed in terms of MFMM with SRWLS and RSS-SDP. In this case, to study the performance of the methods intuitively, we conduct the simulation of RMSE versus variable σ^2, referred to as Fig. 6. With the robust function involved, the performance of RNLA and SRWLS, two methods that convert the problem into a generalized trust-region subproblem, comes closely, albeit the divergence of RNLA and SRWLS is relatively large in Fig. 3. It is worth noting that the margin of the performance among MFMM and others in Fig. 6 is more sizeable than that of Fig. 3.

The RMSE versus variable anchors is depicted in Fig. 4. The performance of all approaches is improved on the rise in the number of anchors. This is because the available information increases when the number of anchors grows. From Fig. 4, we can see that MFMM is better than the rest, albeit the performance of MFMM is worse than RSS-SDP when $M = 4$.

The cumulative distribution function (CDF) of the algorithms is shown in Fig. 5. It can be seen that MFMM achieves $\|\widehat{\boldsymbol{x}} - \boldsymbol{x}\| = 0.73$ m at almost 90%, whereas SRWLS, RSS-SDP, ASM, RNLA and LS achieve $\|\widehat{\boldsymbol{x}} - \boldsymbol{x}\| = 1.1$ m, $\|\widehat{\boldsymbol{x}} - \boldsymbol{x}\| = 1.48$ m, $\|\widehat{\boldsymbol{x}} - \boldsymbol{x}\| = 1.89$ m, $\|\widehat{\boldsymbol{x}} - \boldsymbol{x}\| = 3.47$ m, $\|\widehat{\boldsymbol{x}} - \boldsymbol{x}\| = 4.47$ m at the same probability, respectively.

The outperformance of MFMM can be explained to some extent by the facts that 1) a relatively satisfied initial point is obtained via the first phase optimization (ASM), and 2) the min-max strategy based on Taylor linearization approximation solves the problem with a sequence of convex problems in the second phase of optimization. Specifically, in the first phase optimization, two rounds of procedures are involved, i.e., the feasibility (outer loop) and the optimality (inner loop). Although a similar LS approximation is used in the feasibility, compared with LS in [12], the optimality procedure could further filter out the infeasible points beyond the constraint. Therefore, ASM seems to have a relatively better performance than LS. However, the solution is a local minimum due to the nature of the LS approximation, which drives the second phase of optimization. In the second phase, the optimization is solved with a sequence of convex problems via Taylor linearization, which has a strong property of convergence with a good initial point. For these reasons, MFMM could have a relatively robust and better performance than others in different scenarios.

V. Conclusion

In this letter, a novel localization approach, MFMM, was proposed in the presence of UTP using RSS measurements. Unlike the previous works, a method, i.e., MFMM, with less computational complexity on the precise of high localization accuracy, was taken here. The localization problem was solved under the ANCLS framework by exploiting the ASM integrated with the min-max strategy, which divided the function into a convex quadratic plus a concave term. Simulations demonstrate that MFMM, to some extent, outperforms the other state-of-the-art approaches in different scenarios.

References

[1] N. Saeed, H. Nam, T. Y. Al-Naffouri, and M.-S. Alouini, "A state-of-the-art survey on multidimensional scaling-based localization techniques," *IEEE Commun. Surveys Tuts.*, vol. 21, no. 4, pp. 3565–3583, 4th Quart., 2019.

[2] M. Z. Win, Y. Shen, and W. Dai, "A theoretical foundation of network localization and navigation," *Proc. IEEE*, vol. 106, no. 7, pp. 1136–1165, Jul. 2018.

[3] H. Wu, X. Mei, X. Chen, J. Li, J. Wang, and P. Mohapatra, "A novel cooperative localization algorithm using enhanced particle filter technique in maritime search and rescue wireless sensor network," *ISA Trans.*, vol. 78, pp. 39–46, Jul. 2018.

[4] S. Tomic, M. Beko, and R. Dinis, "3-D target localization in wireless sensor networks using RSS and AoA measurements," *IEEE Trans. Veh. Technol.*, vol. 66, no. 4, pp. 3197–3120, Apr. 2017.

[5] X. Mei, H. Wu, J. Xian, B. Chen, H. Zhang, and X. Liu, "A robust, non-cooperative localization algorithm in the presence of outlier measurements in ocean sensor networks," *Sensors* , vol. 19, no. 12, p. 2708, 2019.

[6] M. Z. Win, W. Dai, Y. Shen, G. Chrisikos, and H. V. Poor, "Network operation strategies for efficient localization and navigation," *Proc. IEEE*, vol. 106, no. 7, pp. 1224–1254, Jul. 2018.

[7] B. Beck, S. Lanh, R. Baxley, and X. Ma, "Uncooperative emitter localization using signal strength in uncalibrated mobile networks," *IEEE Trans. Wireless Commun.*, vol. 16, no. 11, pp. 7488–7500, Nov. 2017.

[8] H. Ketabalian, M. Biguesh, and A. Sheikhi, "A closed-form solution for localization based on RSS," *IEEE Trans. Aerosp. Electron. Syst.*, vol. 56, no. 2, pp. 912–923, Apr. 2020.

[9] H. Lohrasbipeydeh and T. A. Gulliver, "Unknown RSSD-based localization CRLB analysis with semidefinite programming," *IEEE Trans. Commun.*, vol. 67, no. 5, pp. 3791–3805, May 2019.

[10] R. Niu, A. Vempaty, and P. K. Varshney, "Received-signal-strength-based localization in wireless sensor networks," *Proc. IEEE*, vol. 106, no. 7, pp. 1166–1182, Jul. 2018.

[11] W. Li, L. Wang, M. Xiao, Y. Li, and H. Zhang, "Closed form solution for 3D localization based on joint RSS and AOA measurements for mobile communications," *IEEE Access*, vol. 8, pp. 12632–12643, 2019.

[12] K. Yu, "3-D localization error analysis in wireless networks," *IEEE Trans. Wireless Commun.*, vol. 6, no. 10, pp. 3472–3481, Oct. 2007.

[13] M. Z. Win, R. M. Buehrer, G. Chrisikos, A. Conti, and H. V. Poor, "Foundations and trends in localization technologies—Part I [scanning the issue]," *Proc. IEEE*, vol. 106, no. 6, pp. 1019–1021, Jun. 2018.

[14] M. Z. Win, R. M. Buehrer, G. Chrisikos, A. Conti, and H. V. Poor, "Foundations and trends in localization technologies—Part II [scanning the issue]," *Proc. IEEE*, vol. 106, no. 7, pp. 1132–1135, Jun. 2018.

[15] N. Saraf and A. Bemporad, "A bounded-variable least-squares solver based on stable QR updates," *IEEE Trans. Autom. Control*, vol. 65, no. 3, pp. 1242–1247, Mar. 2020.

[16] G. Cimini and A. Bemporad, "Exact complexity certification of active-set methods for quadratic programming," *IEEE Trans. Autom. Control*, vol. 62, no. 12, pp. 6094–6109, Dec. 2017.

[17] A. Lanza, S. Morigi, I. Selesnick, and F. Sgallari, "Nonconvex nonsmooth optimization via convex–nonconvex majorization–minimization," *Numer. Math.*, vol. 136, no. 2, pp. 343–381, 2017.

[18] A. Beck, *First-Order Methods in Optimization*. Philadelphia, PA, USA: Soc. Ind. Appl. Math., 2017.

[19] M. J. D. Powell and Y. Yuan, "A trust region algorithm for equality constrained optimization," *Math. Program.*, vol. 49, no. 1, pp. 189–211, 1990.

[20] T. Zhang, A. F. Molisch, Y. Shen, Q. Zhang, H. Feng, and M. Z. Win, "Joint power and bandwidth allocation in wireless cooperative localization networks," *IEEE Trans. Wireless Commun.*, vol. 15, no. 10, pp. 6527–6540, Oct. 2016.

[21] S. K. Sengijpta, "Fundamentals of statistical signal processing: Estimation theory," *Technometrics*, vol. 37, no. 4, pp. 465–466, Nov. 1995.